

Comparison of NiCrAl-diatomite, nickel graphite and Ag-Cu alloy thermal spraying

C. Ju^a, Q. Li^b, Z. L. Wang^a, Q. H. Song^a, Z. P. Sun^a, Y. F. Zhang^{a,*}

^a*School of Mechanical & Automotive Engineering, Qilu University of Technology, Shandong Academy of Sciences, Jinan, Shandong, 250353, PR China*

^b*School of Material Science & Engineering, Qilu University of Technology, Shandong Academy of Sciences, Jinan, Shandong, 250353, PR China*

NiCrAl-diatomite coatings, nickel graphite coatings and Ag-Cu alloy coatings prepared by thermal spraying were used to study the reaction mechanism. The compositions of NiCrAl-diatomite, nickel graphite and Ag-Cu alloy powders and coatings were investigated by X-ray diffraction. The powders were analyzed by thermogravimetric differential thermal analysis and scanning electron microscopy. The powders and coatings were compared and found to have the same phase by X-ray diffraction. Thermogravimetric differential thermal analysis of the powders showed that NiCrAl-diatomite was almost stable below 800 °C. Ag-Cu alloy coating and nickel graphite coating cannot be used at temperatures above 700 °C and 400 °C, respectively.

(Received March 1, 2021; Accepted July 3, 2021)

Keywords: NiCrAl-diatomite, Nickel graphite, Ag-Cu alloy, Thermal spraying, Coating

1. Introduction

In order to achieve the overall goal of aero engine design and manufacturing, the aircraft engine must achieve the standards of high efficiency and low fuel consumption. One of the important measures to improve engine efficiency is to use sealing coating. The sealing coating should have good surface quality, excellent wear resistance, thermal stability, small friction coefficient and good adhesion to the substrate [1-5]. Nowadays, NiCrAl-diatomite, nickel graphite and Ag-Cu alloy coatings are widely used as abrasion-resistant sealing coatings. Among them, NiCrAl-diatomite are mainly used in high temperature environments. Nickel graphite coating and Ag-Cu alloy coatings can be used for a long time at temperature below 480°C, and the maximum temperature of short-term use can reach 600 °C [6-9]. At present, there is no public report about the comparison of phase analysis and thermogravimetric differential thermal analysis (TG-DTA) of these three kinds of powders and coatings. In fact, studying the changes after thermal spraying can better understand the reaction mechanism of the spraying process, so as to find the best parameters, which can provide a basis for subsequent applications.

* Corresponding author: zhangyanfei@qilu.edu.cn

2. Material and methods

2.1. Material

The NiCrAl-diatomite powders (CM46-2) were supplied by Institute of process engineering, Chinese Academy of Sciences (Beijing, China). The nominal composition of CM46-2 is Ni-60~80%, Cr-8~12%, Al-3.5~5%, the remainder is diatomite. The powder particle size is -150 ± 75 μm . The nickel graphite powders (Metco 307NS) were supplied by Oerlikon Metco (Winterthur, Switzerland). Metco 307NS prepared by chemically clad method, has a particle size of -90 ± 30 μm and a composition ratio of 75% nickel + 25% graphite. The Ag-Cu alloy powders (KF-350) were supplied by GRIMM Technology Group (Beijing, China). The nominal composition of KF-350 is Ag-70.5~73.5%, the remainder is Cu. The powder particle size is -150 ± 60 μm .

2.2. Experimental procedure

Before spraying, the surface of annealed 45 steel (HRC22~25) were cleaned by acetone and then sand blasted with corundum grits. As for Metco 307NS and KF-350, bond coats were plasma sprayed with commercial Metco 450NS powders from Oerlikon Metco. As for CM46-2, the bond coat was plasma sprayed with commercial Amdry 997 from Oerlikon Metco. Afterwards, the NiCrAl-diatomite powders and nickel graphite powders were deposited onto the surfaces of the bond coats using the powder flame spraying process. The Ag-Cu alloy coatings were sprayed by atmospheric plasma sprayed (APS) process. Table 1 and Table 2 show the parameters used.

Table 1. Powder flame spraying parameters of CM46-2 and Metco 307NS.

| Powder | CM46-2 | Metco 307NS |
|----------------------------|--------|-------------|
| Powder delivery | 75 | 70 |
| Oxygen pressure (PSI) | 30 | 30 |
| Oxygen flow rate (SCFH) | 82 | 93 |
| Acetylene pressure (PSI) | 15 | 15 |
| Acetylene flow rate (SCFH) | 49 | 51 |
| Nitrogen pressure (PSI) | 52 | 55 |
| Nitrogen flow rate (SCFH) | 12 | 12 |
| Spraying distance (mm) | 190 | 220 |

Table 2. APS parameters of the KF-350.

| Powder | KF-350 |
|---|--------|
| Current (A) | 500 |
| Voltage (V) | 55 |
| Primary gas pressure (Ar, PSI) | 75 |
| Secondary gas pressure (H ₂ , PSI) | 50 |
| Argon flow rate (SCFH) | 105 |
| Powder feed air flow rate (NLPM) | 8.2 |
| Spray distance (mm) | 110 |

TG-DTA of powder was performed on a STA 449F3 synchronous thermal analyzer (NETZSCH, Germany). The X-ray diffraction (XRD) patterns of the samples were obtained on D8-ADVANCE (AXS, Germany). The morphologies and microstructures of the powders and coatings were evaluated by scanning electron microscopy (SEM, GeminiSEM 500, Carl Zeiss, Germany). The powders and coatings were impregnated with epoxy. After hardening of the resin, the sample was ground with SiC abrasive paper and polished on soft disks with diamond suspension. A cross section of the sample was investigated by SEM and Digital Microscope VHX-5000 (KEYENCE, Japan).

3. Results and discussion

3.1. Powders structure and composition

3.1.1. CM46-2

Figure 1 shows the surface morphologies of the NiCrAl-diatomite powders. The powders have regular spherical shape. Energy dispersive spectrometer (EDS) element mapping (Figure 1e) shows that powder surface shells are NiCrAl alloys, which indicate diatomites cores are encapsulated in NiCrAl alloys shells. It can be seen that the powders have good cladding effect.

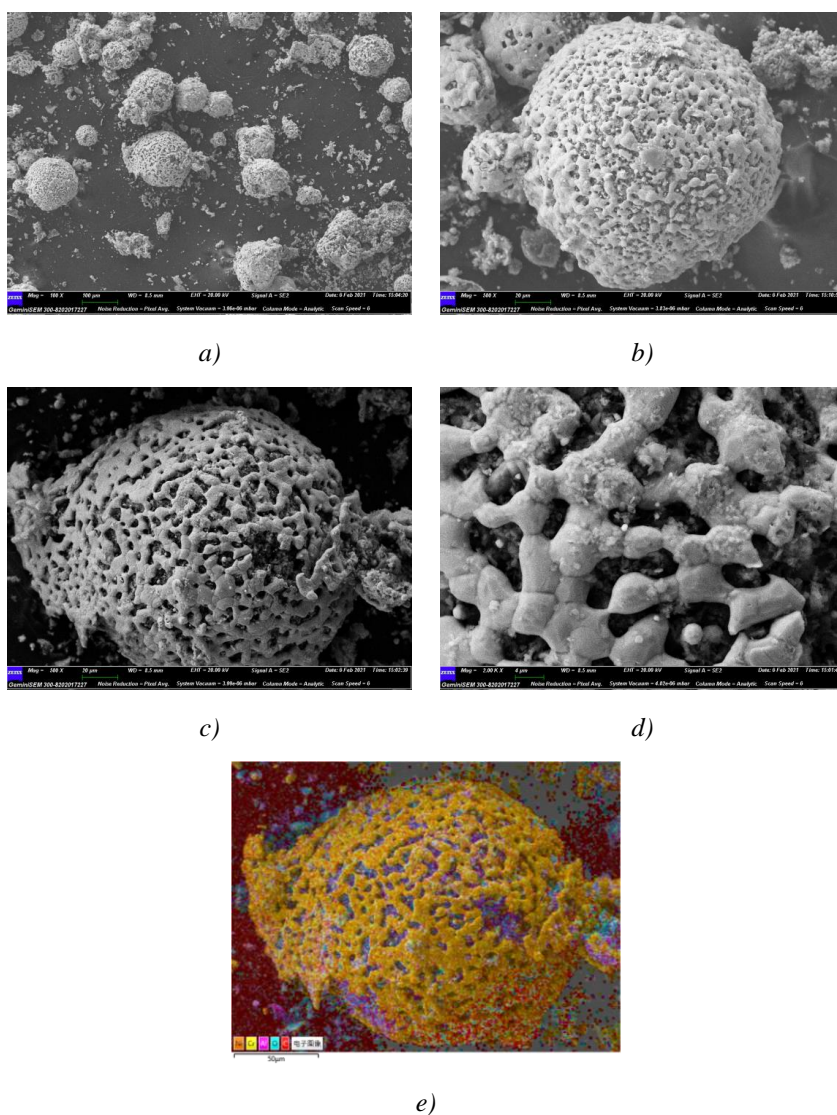


Fig. 1. The surface morphology of CM46-2 composite powders.

The NiCrAl-diatomite powder is made of Ni/diatomite by wet hydrogen reduction liquid phase metal deposition technology, and then made into NiCrAl-diatomite through a high-temperature aluminum-chromium co-infiltration process ^[10]. Therefore, the powder has good oxidation resistance, corrosion resistance and wear resistance.

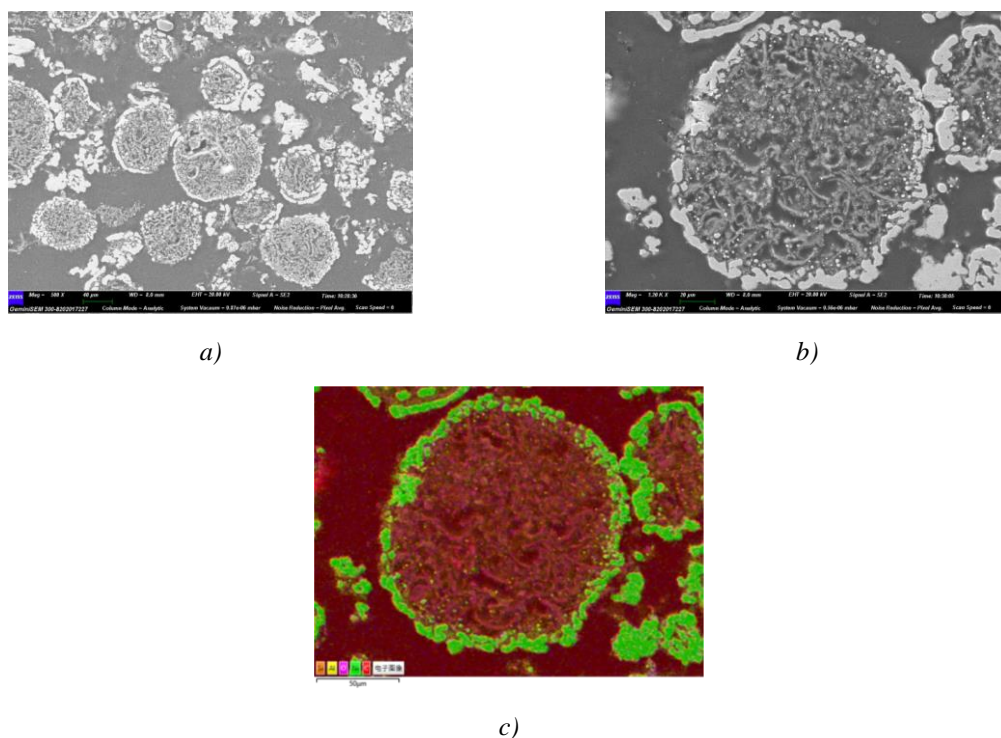


Fig. 2. Cross section of NiCrAl-diatomite powders.

Cross section of NiCrAl-diatomite powders are shown in Figure 2. An obvious cladding structure can be seen, and the powder cross-sectional shape is regular and circular. EDS element mapping in Figure 2c indicates that the powder core is mainly composed of loose and porous diatomite filler, with NiCrAl alloy shell on the surface. Further EDS results indicate that the diatomites are made of SiO_2 , Al_2O_3 , Fe_2O_3 , CaO , Na_2O , K_2O and other elements.

3.1.2. Metco 307NS

The surface morphology of the nickel graphite powder is shown in Figure 3. The nickel graphite particles used in this work are irregular flakes shaped (Figure 3a-c). EDS element mappings (Figure 3e-f) show that the outer surface of the Metco 307NS is mainly composed of metallic Ni. It can be seen that the cladding effect of Ni on the graphite surface is very well, and thus a high quality composite powders can be obtained. Only a small part of powders were not completely coated (Figure 3c-d).

In order to reduce the ablation of graphite in oxidizing atmosphere, the Ni/C preparation methods mainly include wet pressurized hydrogen reduction, carbon-based nickel decomposition, chemical vapor deposition, sol-gel, chemical plating, ion plating, vacuum evaporation, sputtering, physical vapor deposition and electrophoretic deposition ^[11-12]. In this work, Metco 307NS

powders are manufactured by pressurized hydrogen reduction (hydrometallurgy autoclave process) that encapsulates the graphite core inside a nickel shell to form a continuous cladding. This provides a high-quality binder-free composite powders with no tendency for segregation during transport, storage or spraying.

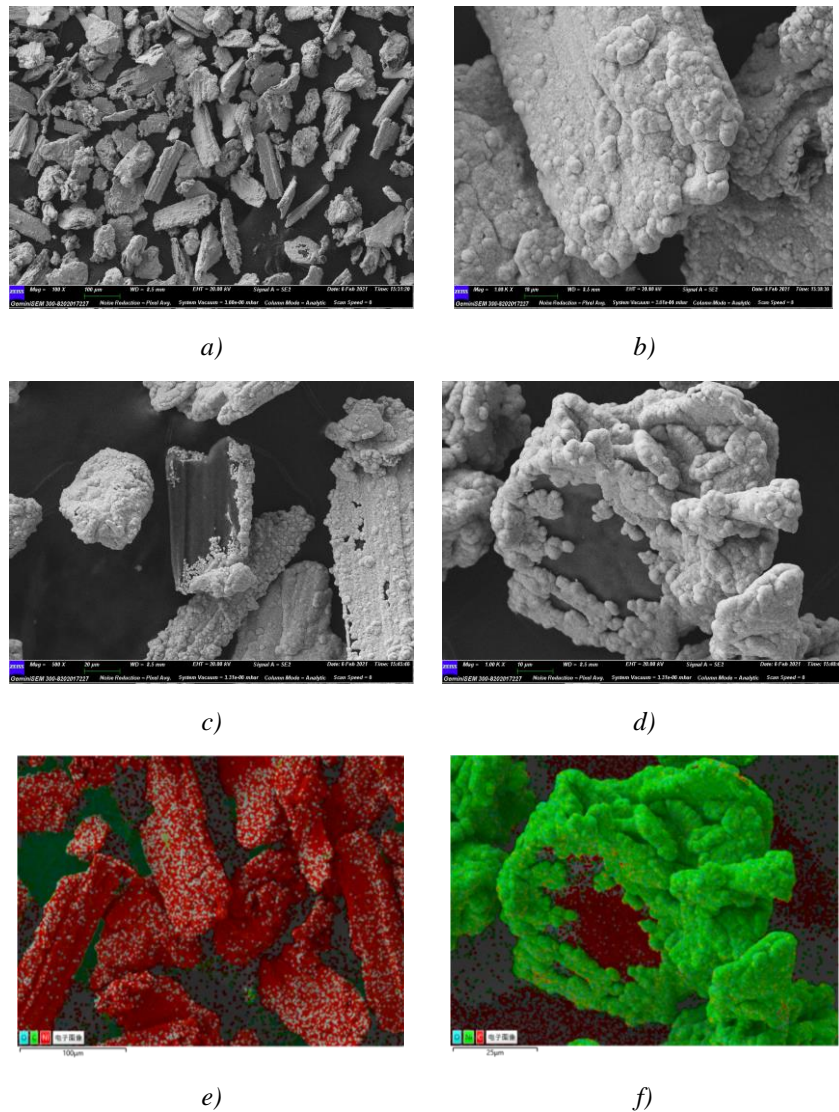


Fig. 3. The surface morphology of nickel graphite composite powders.

Cross section of nickel graphite powders are shown in Figure 4. It can be seen that the powder cross-section shows a irregular shape. A crosssectioned particle in Figure 4b shows the graphite core “A” and the surrounding nickel cladding “B”. It is proved that nickel graphite powders are completely coated by cladding. EDS element mapping (Figure 4c) shows that element contained on the powder surface is basically Ni. The graphite core is wrapped in a nickel shell to form a continuous cladding.

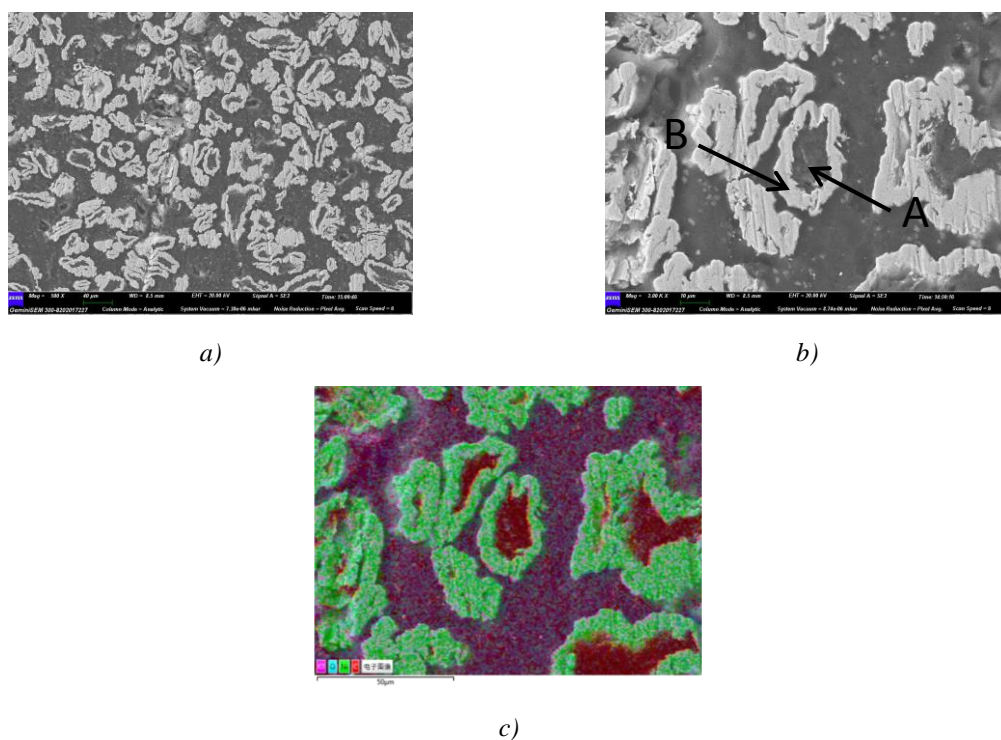


Fig. 4. Cross section of nickel graphite powders.

Manufactured using the hydrometallurgy process, the chemically clad composite particles in these materials demonstrate consistent chemistry and nickel shell thickness surrounding the graphite core. Due to the graphite is easy to be oxidized and ablated. If the spraying material with nickel-graphite phase is used directly, the oxidation ablation rate of graphite will be over 80%, which will greatly reduce the coating performance. Therefore, the surface of the Metco 307NS prepared by chemical cladding method is entirely Ni, and this will increase the antioxidant capacity of the powder.

3.1.3. KF-350

The surface morphology of KF-350 composite powder is shown in Figure 5. It can be seen that the powder particles are mainly spherical, and some small spherical particles adhere to the surface of large spherical particles.

The powders were prepared by gas atomization. The spherical powder particles have good fluidity and can improve the melting effect of particles, and the better the sphericity, the more stable the spraying process, the higher the spraying efficiency, the higher the coating cladding rate, the less the pores and cracks, and the better the performance of the coating [13-14].

The chemical compositions of powders A and B in Figure 5e-f are listed in Table 3 and Table 4. EDS shows that the main elements are silver and copper, and there is a trace of oxygen. The existence of oxygen is mainly due to the oxidation of alloy. And the main oxidized element is copper. Because silver is not easy to be oxidized and pure copper is easy to be oxidized. It can also be seen that the chemical compositions of A and B regions are different. The content of oxygen in small particles is more than that in large particles, and the content of silver is higher.

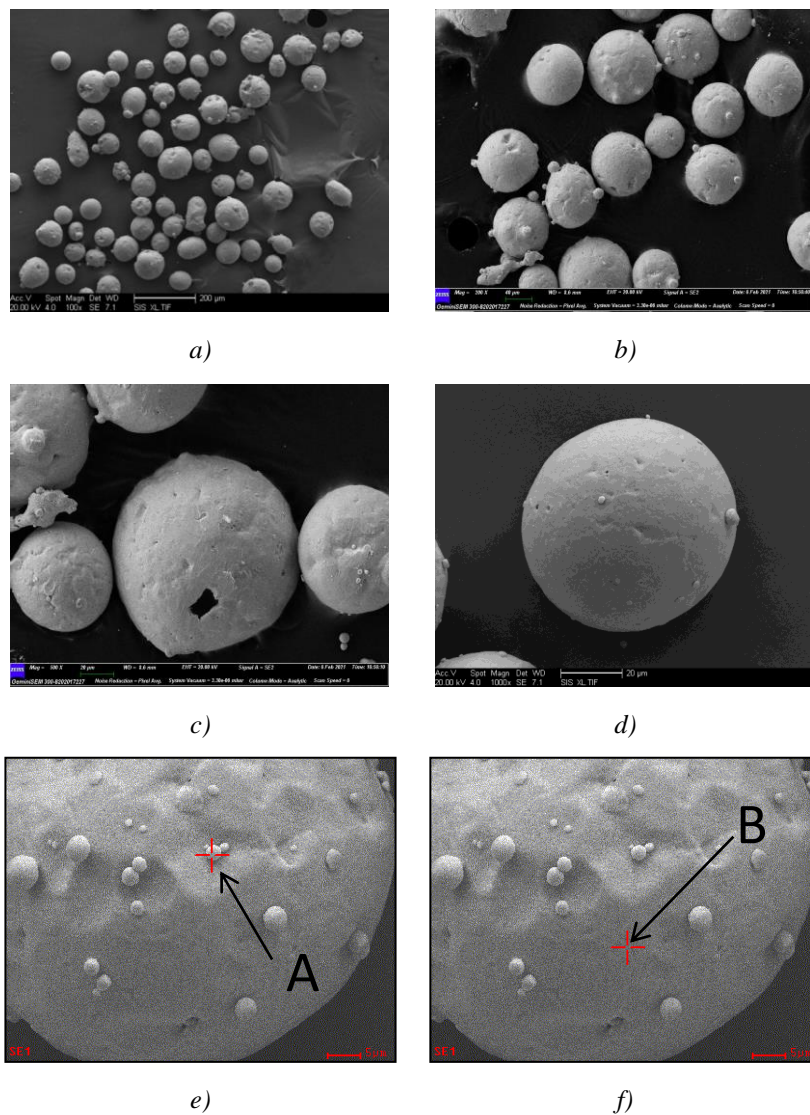


Fig. 5. The surface morphology of KF-350 powders.

Table 3. Chemical compositions of region A in the Fig. 5e.

| Element | OK | AgK | CuK | Matrix |
|---------|-------|-------|-------|------------|
| Wt% | 03.54 | 64.73 | 31.73 | Correction |
| At% | 16.76 | 45.43 | 37.81 | ZAF |

Table 4. Chemical compositions of region B in the Fig. 5f.

| Element | OK | AgK | CuK | Matrix |
|---------|-------|-------|-------|------------|
| Wt% | 01.76 | 59.52 | 38.72 | Correction |
| At% | 08.65 | 43.41 | 47.94 | ZAF |

Cross section of Ag-Cu alloy powders are shown in Figure 6. It can be seen that the powder cross-section shows a regular round shape with uniform size distribution, and the powder

has good fluidity. The powder can improve the efficiency and melting effect in the spraying process, and then improve the performance of the coating.

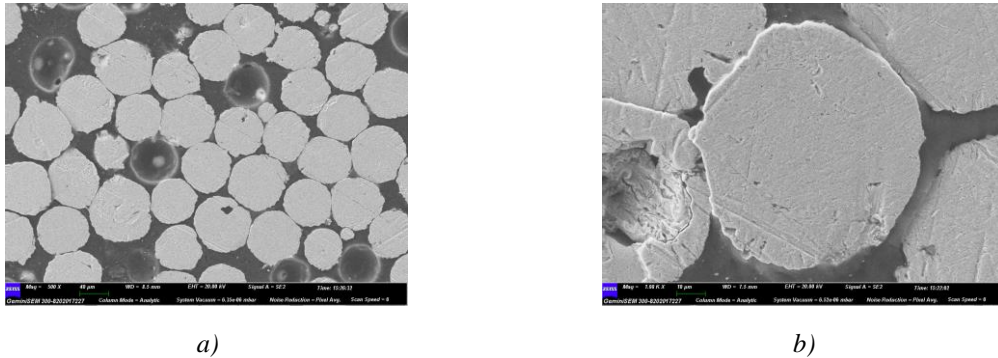
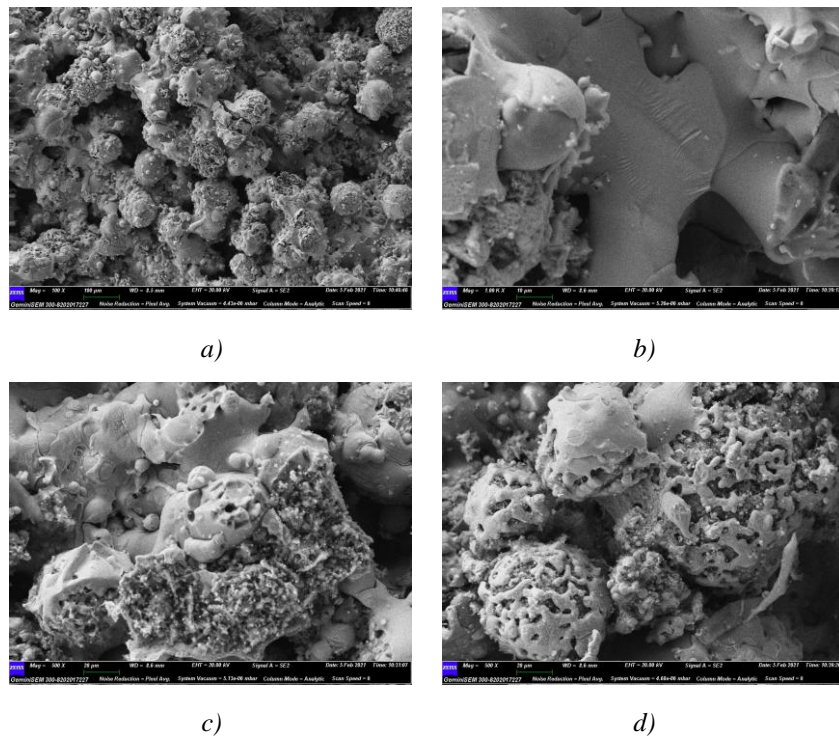


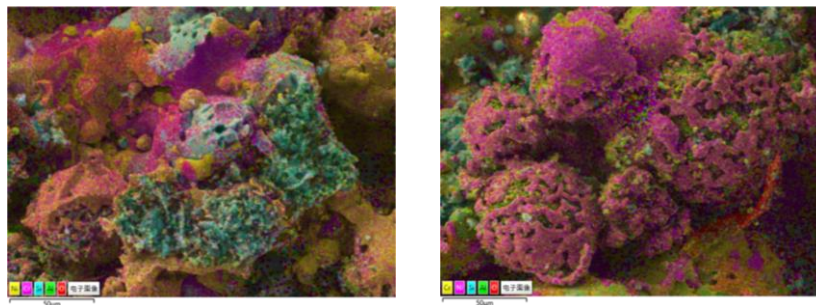
Fig. 6. Cross section of Ag-Cu alloy powders.

3.2. Structure and composition of the coating

3.2.1. CM46-2 coating

The surface morphologies of CM46-2 coatings are shown in Figure 7. The surface of the NiCrAl-diatomite coating is rough and uneven, with more unmelted particles. During flame spraying only part of the outer NiCrAl alloys shells were melted and bond together (Figure 7a-b), most of the NiCrAl-diatomite powders were unmelted and their original spherical structures were preserved (Figure 7d), because flame temperature of flame spraying is lower than that of plasma spraying. Parts of diatomite particles were broken during spraying (Figure 7c). The existence of pores and unmelted particles can reduce the hardness of the coating and improve the grindability of the sealing coating. It can be seen from the EDS element mappings (Figure 7e-f) that the surface of the coating is mainly NiCrAl alloy.

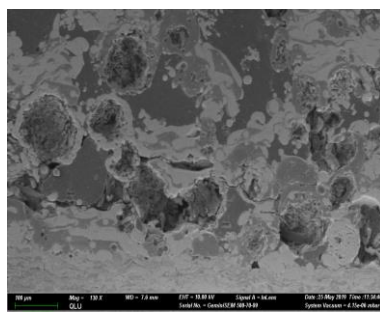




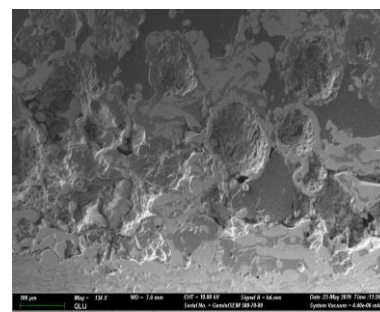
e)

f)

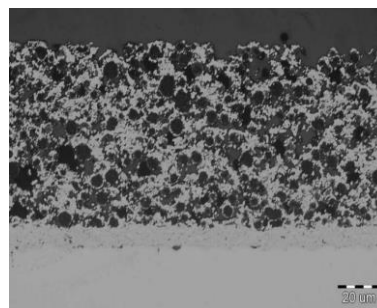
Fig. 7. Surface morphology of CM46-2 coating.



a)



b)



c)

Fig. 8. Cross-section of CM46-2 coating.

Figure 8 shows the cross-section of the CM46-2 coating, the grey areas are NiCrAl metals while the black areas are diatomite, and the spheres of the grey shell encasing the black material are unmelted particles. Most of the diatomites filler cores are still encapsulated in NiCrAl alloys in the coating. The diatomite and the alloy phase are evenly distributed, and it can be seen that there are pores in the coating. This is due to the low temperature of flame spraying, some unmelted particles exist during the spraying process, and the unmelted particles cannot be fully spread out when hitting the substrate, so the coating is easy to produce pores.

In NiCrAl-diatomite coating the metallic phase provides a framework and support function in the coating structure. The diatomite acts to increase porosity, reduce hardness, and enhance grindability. The presence of pores reduces the effect of internal stresses in the coating.

3.2.2. Metco 307NS

Figure 9 shows surface morphology of nickel graphite coating, which is similar to that of NiCrAl-diatomite coatings. The surface of the coating is loose and porous due to low flame spraying temperature and flame flow rate. During flame spraying only part of the outer nickel shells were melted and bond together (Figure 9a-c), most of the nickel graphite powders were unmelted and their original irregular flakes shaped structures were preserved (Figure 9b-d), because flame temperature of flame spraying is lower than that of plasma spraying. Figure 9c shows that the metallic Ni has low surface tension after melting and can spread out well with a smooth surface. Parts of graphite particles were broken during spraying (Figure 9c-d). The existence of pores and unmelted particles can reduce the hardness of the coating and improve the grindability of the sealing coating. It can be seen from the EDS element mapping (Figure 9d) that the surface of the coating is mainly nickel. Ni may be partially oxidized during spraying [15].

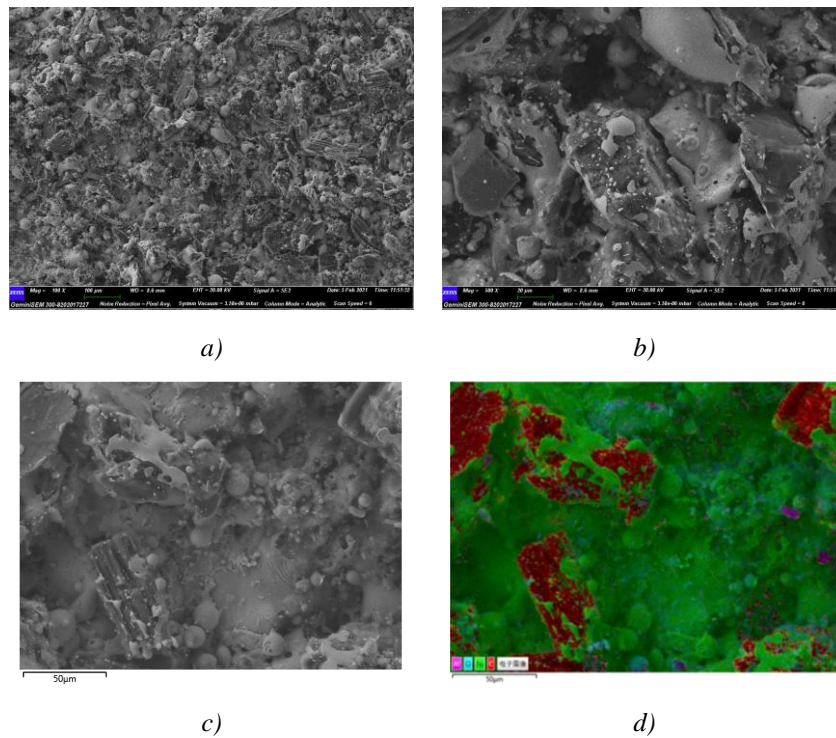


Fig. 9. Surface morphology of nickel graphite coating.

As shown in Figure 10, the grey area of Metco 307NS coating is mainly metallic phase. Metallic nickel has certain strength, toughness and corrosion resistance, which plays the role of skeleton support in the coating. The black area is graphite, which is soft, with good solid lubrication and low thermal expansion coefficient, and plays the role of lubrication and grinding in the coating. Most of the graphites are still encapsulated in Ni in the coating. The presence of nickel increases the bonding strength between graphite and the substrate, which makes graphite not easy to peel off in the friction process.

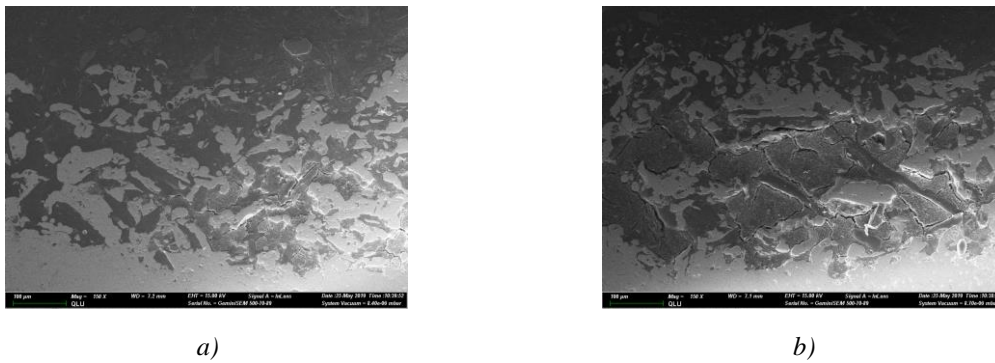


Fig. 10. Cross section of nickel graphite coatings.

3.2.3. KF-350

As shown in Figure 11, the Ag-Cu coating is a typical plasma-sprayed coating. It has honeycomb pores (Figure 11b-c), which are mainly caused by the air mixing in the spraying process.

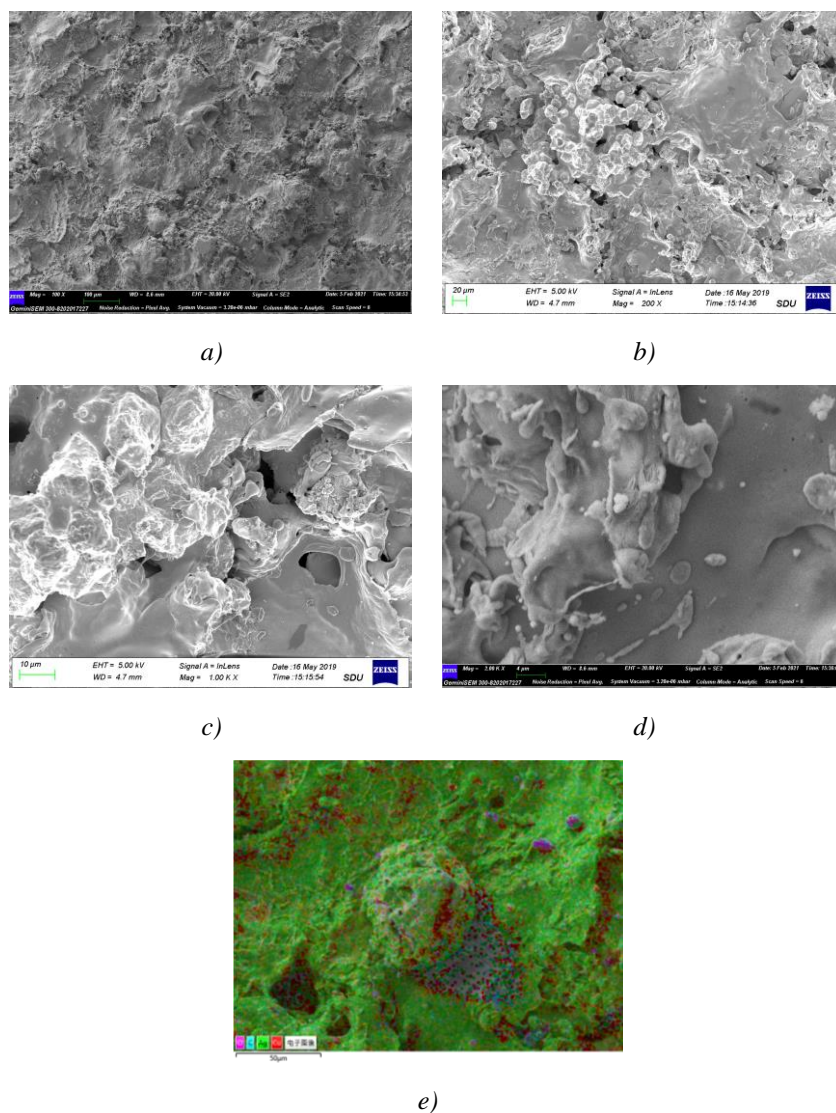


Fig. 11. Surface morphology of KF-350 coating surface.

In the solidification process of the coating, the gas has no time to overflow, so the pores are formed. EDS element mapping (Figure 11e) shows that a small amount of oxidation occurs in the coating.

In the spraying process, inert plasma flame is involved in the air, and the particles on the surface of silver copper coating are heated by high temperature plasma and contact with oxygen in the air, resulting in a small amount of oxidation. The presence of oxide inclusions will adversely affect the performance of the sealing coating, such as reducing the bond strength of the coating and increasing the hardness^[16-17].

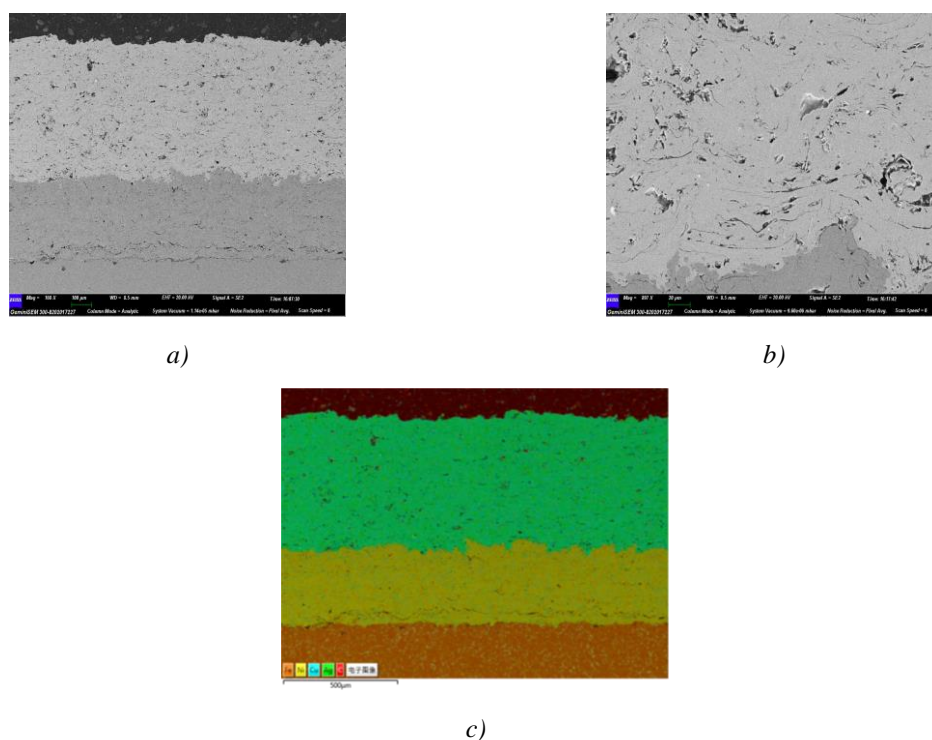


Fig. 12. Cross section of KF-350 coating.

Cross section of KF-350 coating is shown in Figure 12. The typical coating structure of plasma sprayed Ag-Cu coating is lamellar structure, which has obvious micro defects such as pores and cracks. The reason for the existence of pores and microcracks (Figure 12b) is that in the process of spraying, the gas is involved and the molten or semi molten particles are randomly overlapped, which will cause pores, cracks and other micro defects. The coating is closely bonded, and no obvious cracks appear at the interface between Ag-Cu coating and bond coat. It can be seen from the EDS element mapping (Figure 12c) that Ag and Cu are evenly distributed in the coating.

3.3. Phase of coatings and powders

3.3.1. CM46-2

Figure 13 shows the XRD spectra of CM46-2 coating and powder. The XRD spectra of CM46-2 powder and coating match well with Ni (PDF#89-7128), and the intensity of the peaks has weakened after spraying.

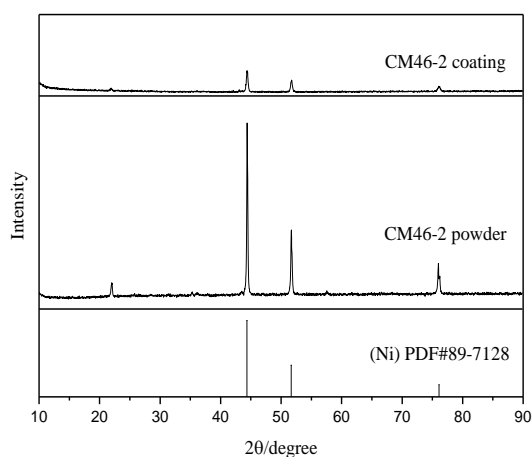


Fig. 13. XRD patterns of the CM46-2 coating and powder.

The NiCrAl-diatomite powder is made of Ni/diatomite by wet hydrogen reduction liquid phase metal deposition technology, and then made into NiCrAl-diatomite through a high-temperature aluminum-chromium co-infiltration process. As shown in Figure 1e, the outer surface of the NiCrAl-diatomite is Ni, so it can be detected with XRD. While diatomites are encapsulated in alloys shells, so diatomites can not be detected with XRD.

After flame spraying, only part of the outer alloys shells were melted and bond together (Figure 7a-b), most of the NiCrAl-diatomite powders were unmelted and their original spherical structures were preserved (Figure 7d). The surface of the coating is mainly alloy, so the XRD pattern of coating is similar to that of the powder. Amorphous phases are formed during spraying so the intensity of the peaks has weakened after spraying.

3.3.2. Metco 307NS

Figure 14 shows the XRD patterns of the Metco 307NS coating and powder, as well as the standard card for Ni (PDF#70-0989) as a reference. The XRD spectrum of the Metco 307NS powder shows that the powder contains only nickel and graphite. The XRD spectrum of the coating shows that the coating is mainly nickel and graphite, with oxide of Ni, indicating Ni played a protective role during the spraying process.

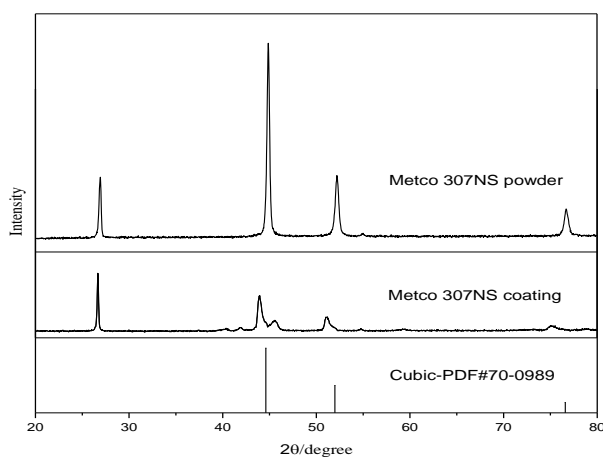


Fig. 14. XRD patterns of the Metco 307NS coating and powder.

3.3.3. KF-350

Figure 15 shows the XRD patterns of KF-350 coating and powder, as well as the standard card of Ag (PDF#87-0720) and Cu (PDF#70-3039) as a reference. The XRD results in Figure 15 show that the powder consists mainly of Ag and Cu. The coating consists mainly of Ag. The decrease of Cu content in the coating is due to the oxidation of Cu in air. This is consistent with the previous EDS analysis results.

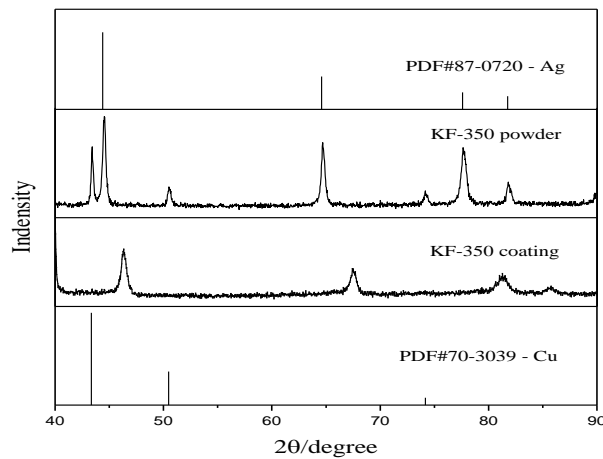


Fig. 15. XRD patterns of the KF-350 coating and powder.

3.4. TG-DTA

3.4.1. CM46-2

Figure 16 shows the TG-DTA curves of the CM46-2 powders in the air. The melting points of Ni, Cr and Al are 1455 °C, 1857 °C and 660 °C, respectively. The melting points of diatomite is about 1650-1750 °C. The powder is almost stable below 800 °C. The reason for the weight gain from 407 °C may be the oxidation of the NiCrAl alloy. Above 1000 °C powder weight increase dramatically indicating serious oxidation. The exothermic peak at 1307 °C is probably due to the phase transformation and thermal decomposition of Al_2O_3 and other oxides in the diatomite.

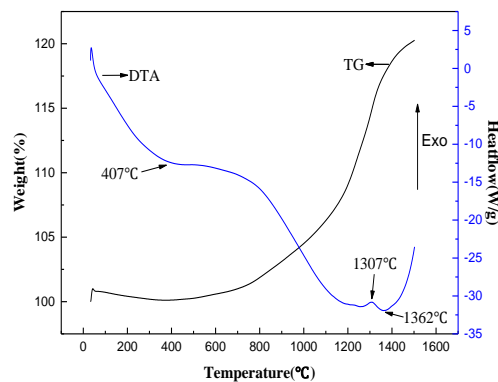


Fig. 16. TG-DTA curves of CM46-2 powders.

3.4.2. Metco 307NS

Figure 17 shows the TG-DTA curves of the Metco 307NS powders in air. From the TG curve, it can be seen that the powder weight increases for about 2% from 394 °C to 754 °C. The weight increase is due to the oxidation of Ni. From 754°C to 1021 °C, the powder loses about 8% of weight, which may be due to the thermal decomposition of graphite. The exothermic peak at 855 °C corresponds to the thermal decomposition of graphite.

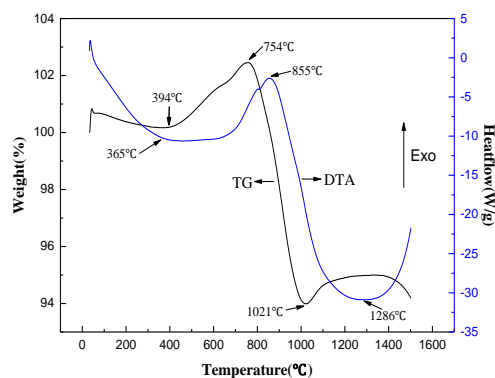


Fig. 17. TG-DTA curves of Metco 307NS powders.

3.4.3. KF-350

Figure 18 shows the TG-DTA curves of the Ag-Cu powders in the air. The melting points of Ag and Cu are 961.78 °C and 1083.4 °C, respectively. The endothermic peak at 784 °C of the DTA curve corresponds to the melting of Ag-Cu alloy.

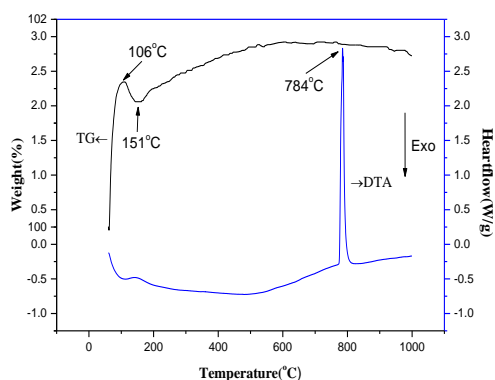


Fig. 18. TG-DTA curves of Ag-Cu alloy powders.

4. Conclusions

In summary, SEM, XRD and TG-DTA were performed to compare the reaction mechanism of NiCrAl-diatomite, Ag-Cu alloy and nickel graphite during thermal spraying. The phase composition and morphology of the powder and coating were analyzed. The following conclusions can be drawn:

(1) The cladding type structure adopted by NiCrAl-diatomite and nickel graphite can well protect the non-metallic materials in the core from oxidation. Cu is easily oxidized, but the Ag-Cu alloy powder improves the oxidation resistance of Cu and enhances the performance of the powder.

(2) The thermal spraying process used for the preparation of NiCrAl-diatomite and nickel graphite coatings in this experiment is powder flame spraying, which is characterized by relatively low flame flow temperature, and the sprayed powder does not melt completely, so the coating prepared by this method has high porosity and the coating is easy to be ground, while the flame flow temperature of plasma spraying is relatively high, and the sprayed powder melts more fully, so the prepared Ag-Cu alloy coating has low porosity. In sealing coating the metallic phase provides a framework and support function, the non-metallic materials act to increase porosity, reduce hardness, and enhance grindability.

(3) NiCrAl-diatomite is almost stable below 800 °C. Ag-Cu alloy coating and nickel graphite coating cannot be used at temperatures above 700 °C and 400 °C, respectively.

Acknowledgements

This work was supported by “20 Policies about Colleges in Jinan” program (Grant NO: 2019GXRC047) and "migratory bird like" high level talent program in Tianqiao District.

References

- [1] L. Q. Zhu, M. L. Liu, J. H. Wang et al., *Act Aeron Au Tica Et Ast Ronautica Sinic* **21**, 85 (2000)
- [2] J. H. Zhang, X. Lu, Z. P. He et al., *Journal of Materials Engineering* **44**(4), 94 (2016)
- [3] Y. X. Luo, H. R. Peng, J. F. Bao. *Thermal Spray Technology* **10**(1), 48 (2018)
- [4] Z. W. Sun, F. H. Bai, Y. F. Zhang. *Heilongjiang Science and Technology Information* **1**, 73 (2016)
- [5] N. Xu, J. Zhang, C. Z. Zhang et al., *CNTSC*, 27 (2010)
- [6] Soltani. R , Sohi. M. H , Ansari M , et al., *Surface & Coatings Technology* **321**, 403 (2017)
- [7] R.E. Johnston, *Surface & Coatings Technology* **10**(205), 3268 (2011)
- [8] X. J. Yuan, B. L. Zha, X. H. Chen et al., *Journal of Propulsion Technology* **38**(02), 457 (2017)
- [9] H. Liu, H. Y. Ma, Y. C. Zhao et al., *Welding Technology* **40**(3), 13 (2011)
- [10] Q. Cao, Q. L. Li, W. P. Ye et al., *Thermal Spray Technology* **6**(1), 35 (2014)
- [11] L. L. Xu, X. P. Gan, T. C. Yuan et al., *Materials Science and Engineering of Powder Metallurgy* **16**(5), 710 (2011)
- [12] L. S. Ren, M. Li, J. Chi et al., *Transactions of Materials and Heat Treatment* **39**(12), 97 (2018)
- [13] G. Li. *Thermal Spray Technology* **10**(2), 26 (2018)
- [14] X. D. Cheng, Z. B. Gao, Q. L. Li et al., *Surface Technology* **37**(4), 21 (2008)
- [15] J. L. Wu, Z. X. Li, W. G. Zhang. *The Chinese Journal of Process Engineering* **7**(6), 1221 (2007)
- [16] Q. Wei, L. W. Zhang, H. Li et al., *Rare Metal Materials and Engineering* **39**(12), 2137 (2010)
- [17] S. M. Du, J. J. Jin, B. X. Hong et al., *Surface Technology* **44**(6), 1 (2015)